Desalination and Water Treatment
www.deswater.com

doi: 10.5004/dwt.2020.25464

192 (2020) 392–399
July

Filtration of BSA through TiO_2 photocatalyst modified PVDF membranes

Elias Jigar[a,b], Krisztina Bagi[b], Ákos Fazekas[b], Szabolcs Kertész[b], Gábor Veréb[b], Zsuzsanna László[b,c,*]

[a]*Doctoral School of Environmental Sciences, University of Szeged,. H-6720, Rerrich B. tér 1. Hungary, email: eliasjig@gmail.com (E. Jigar)*
[b]*Department of Process Engineering, Faculty of Engineering, University of Szeged, Moszkvai krt. 9, H-6725 Szeged, Hungary, emails: zsizsu@mk.u-szeged.hu (Z. László), bagi.krisztina@hotmail.com (K. Bagi), fazekas.akos92@gmail.com (A. Fazekas), keroszabi@yahoo.co (S. Kertész), verebg@mk.u-szeged.hu (G. Veréb)*
[c]*Institute of Environmental Science and Technology, University of Szeged, H-6720, Tisza Lajos Blvd. 103, Szeged, Hungary*

Received 31 October 2019; Accepted 18 January 2020

ABSTRACT

In this study, composite ultrafilter membranes were prepared by coating Polyvinylidene fluoride [PVDF; molecular weight cut off (MWCO) values of 30 and 100 kDa] with inorganic titanium dioxide (TiO_2) nanoparticles. Hydrophilicity, flux, and rejection performance of the pristine and modified membranes using 1 g/L bovine serum albumin (BSA) under different pH conditions were compared. Reversible and irreversible filtration resistances were calculated and compared using a resistance-in-series model. Regeneration of the fouled modified membrane using ultraviolet (UV) light was also studied. Modified PVDF membrane is found to be very hydrophilic due to the TiO_2 layer, and in the case of 30 kDa membranes, it exhibits higher filtration resistances. As pH increases, the irreversible resistance decreases and is smaller than the reversible resistance due to strong repulsion forces between the BSA-BSA molecules and the BSA-membrane surface. Due to differences in membrane MWCO, the higher rejection was found with the 30 kDa membranes. The surprising result was that the modified TiO_2 layer decreased BSA rejection with enhanced filtration resistance, This could be explained by the presence of TiO_2, which prevents the formation of a gel layer, and/or the nanoparticles may change the protein structure, allowing for permeation. TiO_2-coated PVDF membranes revealed better antifouling properties and cleaning of membranes by exposure to UV light resulted in the recovery of original flux after 3 h (30 kDa) and 2 h (100 kDa), respectively. Although this work could not provide good separation of proteins via the modified membranes, these results reveal the necessity of further investigation into the interactions between proteins and nanoparticles.

Keywords: Fouling; Filtration resistances; BSA; Heterogeneous photocatalysis; Nanoparticles; Titanium dioxide

1. Introduction

The dairy industry is one of the most polluting among the food industries with the most substantial volume of effluent generated, and the highest pollution load [1]. Dairy industrial wastewater contains high concentrations of organic matter and nutrients, which are mainly a combination of carbohydrates, proteins and fats originating from milk, and also residual cleaning agents [2]. Due to the high pollution load of dairy wastewater, discharging untreated/partially treated wastewater harms aquatic and terrestrial ecosystems and results in serious environmental problems. Such problems raise the concern that dairy wastewater needs to be efficiently treated before its discharge to meet ecological discharge standards [3].

In membrane technology, filtration using polymeric membranes has attracted attention due to the ease of operation and integration with other processes, reliable

* Corresponding author.

Presented at PERMEA 2019, 26–29 August 2019, Budapest, Hungary

contaminant removal without the production of any harmful by-products and cost efficiency compared to other inorganic membranes [4]. However, membrane fouling limits the practical application of these techniques [5].

Polyvinylidene fluoride (PVDF) is a widely used organic polymer with excellent thermal stability, mechanical strength and chemical resistance to aggressive reagents like organic solvents, acids, and bases [6]. Due to the hydrophobic nature of PVDF, it has a high fouling tendency when exposed to protein-containing solutions.

A catalytic membrane reactor (CMR) is a composite unit in which membranes and catalysts are joined together. In the established scientific literature, there are four kinds of CMRs in use for wastewater treatment. These are (1) photo-catalytic membrane reactors (PMRs), which are employed by integrating advanced oxidation processes (AOPs) like photocatalysis with membrane technology [7], (2) enzymatic membrane reactors (EMRs), which are a coupling of a membrane separation process with an enzymatic reaction. [8], (3) electro-catalysts, which integrate electrocatalytic reactions and the process of membrane separation into one processing stage [9], and (4) Fenton-based chemical reactors [10]. The reactors mentioned above help improve chemical oxidation of organic pollutants [11] and antimicrobial action [12].

Among the above membrane reactors, the PMRs are promising for the treatment of contaminants due to the potential use of suitable light irradiation to degrade compounds in wastewater into less or non-toxic minerals, such carbon dioxide, ammonia, and water [13].

PMRs can be classified into three types depending on the techniques used to incorporate photocatalytic materials into the membrane. These are (1) photocatalyst-coated membranes, (2) photocatalyst-blended membranes, and (3) self-photocatalytic membranes [14]

Firstly, photocatalyst-coated membranes can be synthesized using various techniques, including dip-coating [15], electrospinning [16], electrospraying [17,16], phase inversion [18–20], advanced atomic layer deposition (ALD) [21], and physical deposition [22].

The sol-gel process of dip-coating uniformly coats the surface of the membrane with the nanomaterial. However, the process includes complicated steps such as drying, binder mixing, coating, and calculations. Moreover, high-temperature calcination cannot be applied to less heat-resistant support materials [15].

Electrospinning is an effective and straightforward method to prepare membranes that have a homogeneous distribution of pores and excellent interconnectivity. However, the lack of upscaling for massive production is the main drawback in the use of this method at a commercial scale [16]. This kind of membrane can also be developed through physical blending [19] and the non-solvent induced phase separation wet-process [23,24].

Electrospraying, also known as electrohydrodynamic atomization, is a method that allows uniform deposition and provides benefits of high deposition efficiency, easy control of film thickness, and low cost [17].

The phase inversion method is a separating process in which a uniform solution of polymer and nanoscale entities is converted into a solid phase in a controlled way. It is usually used to prepare asymmetric polymer nanocomposite membranes (PNCMs) with a thin, dense layer. The critical parameters for membrane preparation are the choice of the polymer solution, solvent, non-solvent, film casting conditions, and coagulation bath composition [23]. However, the benefit of substantial morphological differences can be obtained from this method by changing the parameters.

ALD is one of the physical deposition methods used to develop photocatalytic membranes. Film thickness is easily controlled and coatings can be added using a low temperature with this technique [21].

Physical deposition is a process by which the photocatalyst is suspended in propanol using ultrasonication. The suspension is then filtered through a membrane in a dead-end cell and let air dry at room temperature [22].

Secondly, membranes developed by blending photocatalysts with membrane material offer no leaching of the photocatalyst but suffer from a marginal increase in hydrophilicity and less reproducibility.

Thirdly, unlike coated or blended membranes, self-catalytic membranes do not require any immobilization step and are produced by electrochemical anodization to provide high anatase crystallinity, hydrophilicity, surface area, and nanotubular morphology to create increased photocatalytic efficiency [14].

Photocatalyst-coated membranes have several advantages over the others, as they have higher hydrophilicity, improved anti-fouling properties and help protect ultraviolet (UV) sensitive membranes. Among the techniques used to develop photocatalyst-coated membranes, physical deposition has gained much importance due to its simplicity and reproducibility [25].

Photocatalysis uses light irradiation to activate semiconductor metal oxides, such as titanium dioxide (TiO_2) [22,26], zinc oxide (ZnO) [27], graphene oxide [28], zirconium oxide (ZrO_2) [26,29], aluminum oxide (Al_2O_3) [30], silicate (SiO_2)[31], and tungsten trioxide (WO_3) [32]. Amongst the mentioned photocatalysts, anatase TiO_2 has many advantages over other AOPs and is most widely used due to its availability, high photocatalytic activity, chemical inertness, mechanical strength, non-toxicity, hydrophilicity, photostability, and low cost [33,34].

Several studies revealed differing TiO_2-PVDF composite membrane performance depending on the synthesis of the composite membrane, the concentration of TiO_2, and waste water characteristics. For example, the deposition of TiO_2 enhanced the hydrophilicity and fouling resistance of PVDF membranes by 120 ALD. A study also showed a pore size reduction which explained the improvement in bovine serum albumin (BSA) rejection [21]. A wide range of concentrations (0–30% wt.TiO_2/PVDF) were also used to prepare TiO_2-PVDF composite membranes with the phase inversion method. For low concentrations, no improvement in membrane properties was observed. For intermediate TiO_2 concentrations, permeability, and flux performances increased with increasing TiO_2 content. An optimum value was obtained around 25%wt. Beyond this concentration, TiO_2 agglomeration inside some pores of the membrane may induce a decrease in membrane permeability, but it remained higher than that of the neat PVDF membrane [23].

Another example is an improvement in hydrophilicity and porosity of TiO_2-PVDF mixed matrix membranes, which

resulted in improved water flux and a reduction in BSA rejection [35]. All of the above studies did not indicate that the effect of TiO_2 on model dairy wastewater filtration parameters was a function of pH.

Hence, this study aimed to create a composite PVDF/TiO_2 membrane prepared by physical deposition and to examine the effect of TiO_2 on filtration of BSA model solutions to gain more information about the behavior of protein fouling during membrane filtration of dairy wastewaters. Filtration characteristics were investigated over a wide range of pH with different MWCO membranes. Moreover, the flux recovery of the modified membranes was investigated under UV irradiation.

2. Experimental design

In our study, pristine and modified PVDF ultrafilter (UF) membranes (JW PVDF 30kDa GE Osmonics) and Kynar 400 PVDF 100 kDa molecular weight cut off (MWCO) values were purchased from New Logic Research Inc., USA. As shown in Fig. 1, the membranes were modified using the physical deposition method [22], in which 0.04 g commercial TiO_2 Aeroxide P25 was suspended in 100 ml of i-propanol using ultrasonication, then the suspension was filtered through a membrane in a dead-end cell at 0.3 MPa and let air dry for 1 h at room temperature.

The membrane filtration experiments using 1 g/L BSA [36] were carried out at a pH of 4.7, 6.2, and 8. Buffer solutions were prepared from 0.1 M disodium phosphate (Na_2HPO_4) and 0.1 M sodium dihydrogen phosphate (NaH_2PO_4). The chemicals were analytical grade and purchased from VWR International (VWR International, Hungary). BSA concentration of 1 g/L was used to simulate a similar concentration of proteins in real wastewater.

As indicated in Fig. 2, a 0.0035 m^2 membrane was placed in the bottom of the dead-end cell (Millipore, XFUF04701, USA). The feed (pure water, BSA solution) was filled in the feed tank, where N_2 gas provided the transmembrane

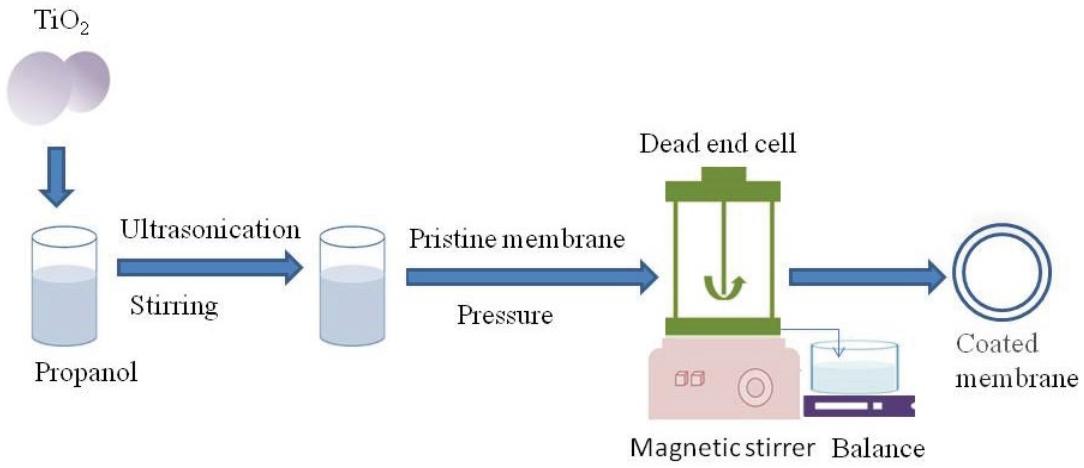

Fig. 1. Scheme of modified membrane synthesis.

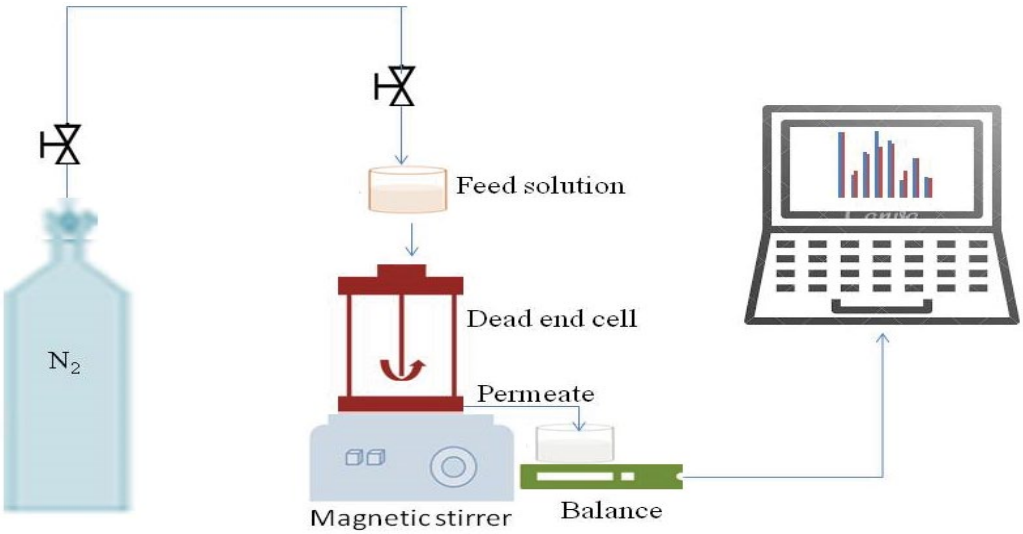

Fig. 2. Schematic representation of the dead-end filtration setup.

pressure and the liquid inside the cell was stirred at 350 rpm. The weight of permeate was recorded by a digital balance during the given period. All membranes were subjected to 250 ml distilled water at 0.2 MPa before the measurements. Subsequently, the pure water flux and rejection tests were performed at 0.1 MPa. In each filtration, 250 mL water or model solution was filtered to volume reduction ratio (VRR) 5. VRR can be calculated using the following Eq. (1):

$$\mathrm{VRR} = \frac{\mathrm{VF}}{\mathrm{VF} - \mathrm{VP}} \tag{1}$$

where VF and VP in the equation are the volume of the feed and permeate [m^3], respectively, at a given time.

2.1. Analytical methods

Standard potassium-dichromate oxidation method was the technique used to determine chemical oxygen demand (COD) in our experiment. About 2 ml of sample was added to standard test tubes (Lovibond) and digestion was carried out in a COD digester (Lovibond, ET 108) for 2 h at 150°C to measure COD values in the COD photometer (Lovibond PC-CheckIt). BSA concentrations in feed and permeate solutions were measured using a spectrometer (Hitachi Co., U-2000, Japan) at 280 nm [37].

Water and permeate fluxes of the neat and modified membranes were compared, organic content (COD), and protein rejection was investigated.

The permeate flux was calculated as:

$$J = \frac{W}{ST} \tag{2}$$

where J represents the permeate flux (kg/m^2h), W represents the mass of permeate water (kg), S represents the effective membrane area (m^2), and T represents the filtration duration.

Rejection was calculated using the following Eq. (3):

$$\mathrm{Rejection}(\%) = \frac{C_0 - C}{C_0} \times 100 \tag{3}$$

where C_0 and C are the concentrations of feed and permeate solutions, respectively.

The filtration resistance was calculated as [22] through the resistance in a series model, as indicated in Table 1.

Contact angles can be measured using the sessile drop method (Dataphysics Contact Angle System OCA15Pro, Germany) [38].

Stability of the modified membrane can be investigated using the mass retention ratio (MR) parameter. To compare it with the original values, we needed to measure the weight change of modified membranes which were rinsed with distilled water in a stirred bath at 150 rpm and 60°C. The MR can be calculated by the following Eq. (4) [39]:

$$M(\%) = \frac{W_t}{W_1} \times 100 \tag{4}$$

Zeta potentials were obtained by computation with the Helmholtz–Smoluchowski (H–S) equation following the experimental measurement of the streaming potential.

Table 1
Filtration resistance formulas[

Filtration resistances	Formula
RM (m^{-1})	$\mathrm{RM} = \frac{\Delta P}{J_w \times \eta_w}$
Rirrev (m^{-1})	$\mathrm{Rirrev} = \frac{\Delta P}{J_w \times \eta_w} - \mathrm{RM}$
Rrev (m^{-1})	$\mathrm{Rrev} = \frac{\Delta P}{J_c \times \eta_{ww}} - \mathrm{RF} - \mathrm{RM}$
Total resistance	$\mathrm{RT} = \mathrm{RM} + \mathrm{Rirrev} + \mathrm{Rrev}$

where Δp = pressure difference between the two sides of the membrane (Pa), J_W = water flux of the clean membrane (L/m^2h), η_W = water viscosity (Pa s), and η_{ww} = wastewater viscosity.

The measurements of streaming potential were performed in the Adjustable Gap Cell of SurPASS 3. Two samples with the same surface were fixed on sample holders with a cross-section of 20 × 10 mm using double-sided adhesive tape. A distance of 110 ± 10 μm between sample surfaces was maintained by continuously decreasing the gap of the flow channel with a micrometer screw integrated into the measuring cell. The surface zeta potential was determined in the presence of 0.001 mol/L KCl solution at various pHs in the range of pH 2.5–8.

The streaming potential was measured within a certain pressure range and the slope of the linear dependence (i.e., the streaming potential coupling coefficient $dU_{str}/d\Delta p$) was used to calculate the surface zeta potential according to the classical Helmholtz–Smoluchowski Eq. (5),

$$\zeta = \frac{dU_{\mathrm{str}}}{\Delta P} X \frac{\eta}{\varepsilon_{\mathrm{rel}} \times \varepsilon_0} \times K_B \tag{5}$$

η and ε_{rel} are the dynamic viscosity and dielectric coefficient of water, ε_0 is the permittivity of free space, and K_B is the electric conductivity of the aqueous solution.

3. Results and discussion

3.1. Stability of the modified membrane

The stability of the TiO_2-coated PVDF membrane by physical deposition was investigated by MR and flux retention ratio (FR) parameters. The results for MR and FR were 98.13% and 99.14%, respectively. There was 40 mg TiO_2 deposited on the membrane. The turbidity value before and after 16 h of washing in 200 ml was 0.601 and 1.55 NTU, respectively, while the turbidity values of 5, 10, and 20 mg TiO_2 in 200 ml were 90.63, 190, and 450.33 NTU, respectively. The change in turbidity of the coated membrane is insignificant when compared with turbidities of 5, 10, and 20 mg TiO_2 solution. Hence the results revealed that the coated membrane is stable.

3.2. Zeta potential of TiO_2-coated PVDF membrane

Strictly linear dependence of streaming potential on the pressure gradient with a coefficient of linear regression was $R^2 > 0.99$, indicating high quality and reliability of the zeta potential analysis. As indicated in Fig. 3, the zeta potential for TiO_2-PVDF membrane shows the IEP at pH 3.6. The zeta potential is negative at neutral pH.

3.3. Water contact angle measurements

Contact angles were measured to study the surface hydrophilicity of the PVDF membrane, and the contact angles formed by distilled water on the surface of pristine and modified PVDF membrane were calculated using mean ± standard deviation (STDEV) of six sample points. The mean ± STDEV of 30 and 100 kDa pristine membrane was 63 ± 2.49 and 51.97 ± 4.37, respectively. However, the contact angle measurement of the coating membranes was difficult to obtain. This implies that TiO_2 made the PVDF membrane very hydrophilic due to its hydroxyl groups. A similar study by Zhao and Yu [38] indicated hydrophilicity improvement of the pristine PVDF membrane by TiO_2.

3.4. Filtration of BSA solution in its native pH

In the first series of experiments, 1 g/L BSA was dissolved in distilled water and filtered through the pristine and modified membranes. Filtration resistances were calculated through the use of formulas in Table 1. The membrane resistance (RM), irreversible resistances (Rirrev), reversible resistances (Rrev), and total resistances (RT) are presented in Figs. 4 and 5. It was found that the modification significantly increased the RM of 30 kD PVDF membranes, while it did not significantly affect RM of 100 kD membranes. Moreover, surprisingly, higher filtration resistances were observed in 30 kD membranes. It was also found that the irreversible fouling of the modified membrane was more significant than reversible fouling and also more significant than the fouling of the pristine membrane. Our results are under the earlier observations [40,41] as increasing TiO_2 loading in the membrane decreases water flux.

The protein and COD rejection of the pristine and modified membranes in the presence or absence of TiO_2 are illustrated in Figs. 6a and b. It was found that the pristine membrane rejects more protein and COD than the modified one. This is a very surprising result taking into consideration that in the case of 30 kD membranes, the modification enhanced filtration resistances, thus it was expected that the enhanced Rirrev and Rrev would lead to increased protein rejection. However, this result is similar to the result obtained by Farahani et.al [35].

Comparing BSA rejection in the cases of 30 and 100 kD membranes (Figs. 6a and b), it was found that the modification slightly decreased BSA retention in the case of the 30 kD membrane, but dramatically decreased it in the case of the 100 kD membrane. One possible explanation may be that a gel layer is formed on the surface of the membrane which enables protein retention, while in the case of a modified surface, the gel layer can not form because of the enhanced hydrophilicity of the membrane surface caused by TiO_2

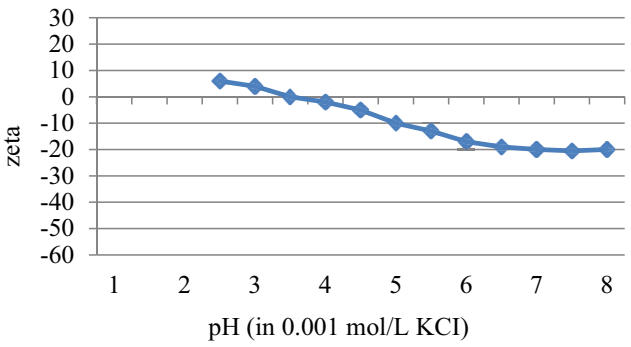

Fig. 3. pH dependence of zata potential for TiO_2 coating PVDF 100 kDa.

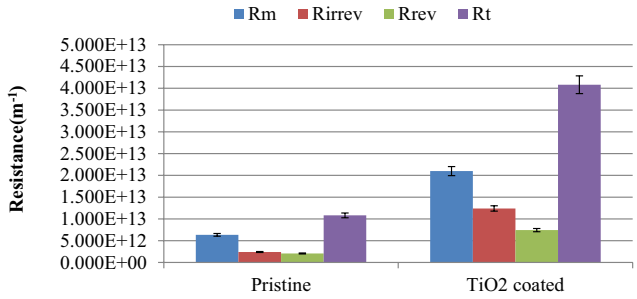

Fig. 4. Filtration resistance of 30 kDa pristine and modified membranes at the natural pH of BSA solution (pH 6).

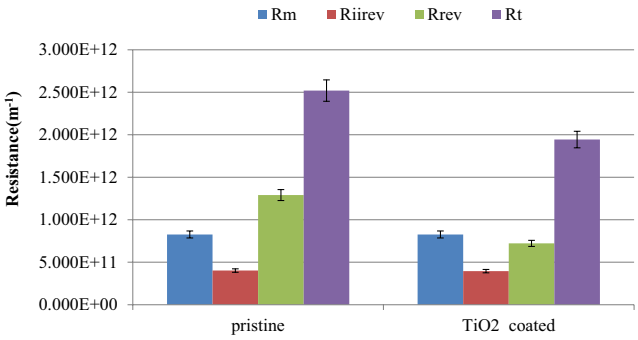

Fig. 5. Filtration resistance of 100 kDa pristine and modified membranes at the natural pH of BSA solution (pH 6).

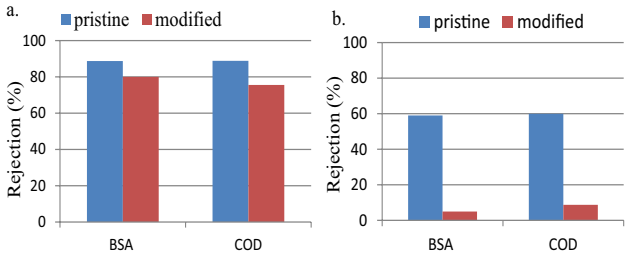

Fig. 6. Rejection of BSA by pristine and modified membranes (a). 30 kDa (b). 100 kD membranes.

particles. However, this explanation is not under the results of 30 kDa membrane filtration; in this case, the filtration resistances are very low compared to RM and lower than measured in the presence of TiO_2; so probably there is no considerable gel layer formation.

This means, that TiO_2 may act on retention in another way and we have to take into consideration the protein-nanoparticle interactions. The adsorption of a protein to a surface is a very complex process, determined by several factors, like electrostatic forces and hydrophobic dipol-dipol interactions. Although the exact description of the mechanisms of adsorption could be achieved by using several different complementary techniques, earlier results make it probable, that the surface of nanoparticles can modify the structure and therefore the behavior and function of the adsorbed protein [42]. Thus, the TiO_2 nanoparticles may cause such changes in BSA structure which results in enhanced permeation through the membrane, which is more expressed in the case of the 100 kD membrane, due to its higher MWCO.

3.5. Effect of pH on BSA filtration

In the next series of experiments, the effect of pH on filtration resistances was investigated in the presence of a phosphate buffer. As indicated in Fig. 7, Rirrev decreases and is smaller than Rrev as pH increases. It can be explained by the higher electro-static repulsion between the surface and the fouling particles, which reduces both the aggregation of BSA molecules and the adsorption of the negatively charged BSA molecules onto the membrane surface [41]. The high filtration resistance and alteration of RM of the modified membrane in the presence of phosphate could be a result of co-adsorbed BSA and phosphate on TiO_2 surface [43].

In case of the 100 kDa membrane, the filtration resistance during BSA filtration is lower than the 30 kDa membrane. In the case of the pristine membrane, as pH increases, the Rrev increases and becomes larger than the Rirrev. In the modified membranes both Rrev and Rirrev decrease as pH increases (Fig. 8). The diminished fouling is probably similar to the results obtained in the absence of buffer, and the explanation can be confirmed by examination of protein rejection (Fig. 9).

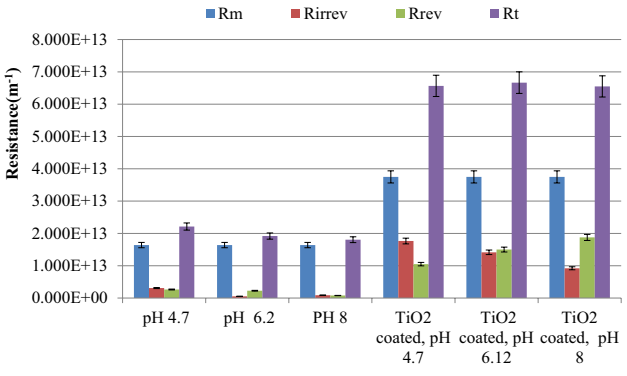

Fig. 7. Effect of pH on BSA filtration resistance through 30 kDa membrane in the presence or absence of TiO_2.

As shown in Fig. 9, rejection in the pristine membrane increased as the pH of the solution increased from pH 4.7 to 8, due to higher electro-static repulsion, which reduces the aggregation ability of BSA molecules and the adsorption ability of the negatively charged BSA molecules onto the membrane surface to form a gel layer [35]. Some authors argue that proteins in solution may aggregate more readily at their isoelectric point, because of reduced electrostatic repulsion, and these aggregates may cause fouling. Besides, proteins at their isoelectric point have smaller sizes than at other values of pH and, therefore, pass simply through the membrane [44]. The effect of pH is greater in the modified PVDF membrane. This could be caused by the impact of co-adsorbed phosphate on the BSA-TiO_2 surface interaction. In this interaction, conformational changes of adsorbed BSA are influenced by phosphate on the TiO_2 surface at pH 7.4 and pH 4.5 [43]. Thus, BSA can easily pass the membrane and reduce rejection.

The effect of pH on rejection during filtration with a 100 kDa membrane, as indicated in Fig. 10, is quite different from that at 30 kDa, in that rejection decreases as pH increases. Proteins at higher pH tend to pass through large MWCO while they form aggregates and cause fouling at lower pH. The higher rejection at lower pH is therefore due to fouling because of smaller electrostatic repulsion forces. The lower rejection at higher pH is due to lower fouling as a result of higher electrostatic repulsion forces [35].

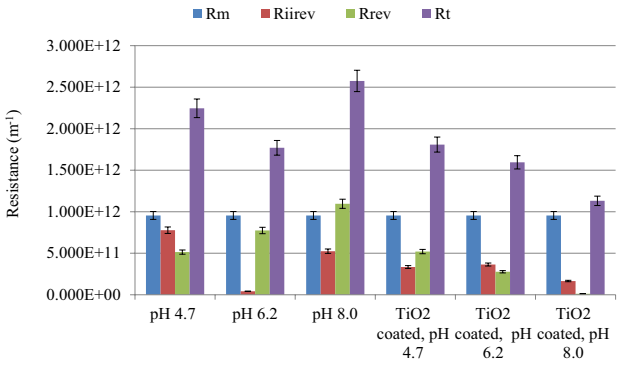

Fig. 8. Effect of pH on BSA filtration resistance through 100 kDa membrane in the presence or absence of TiO_2.

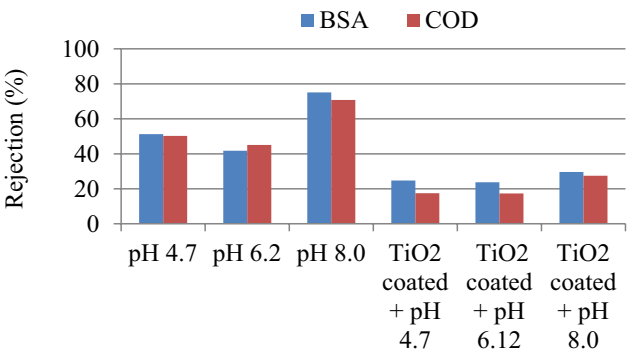

Fig. 9. Effect of pH on rejection for 30 kDa BSA filtration.

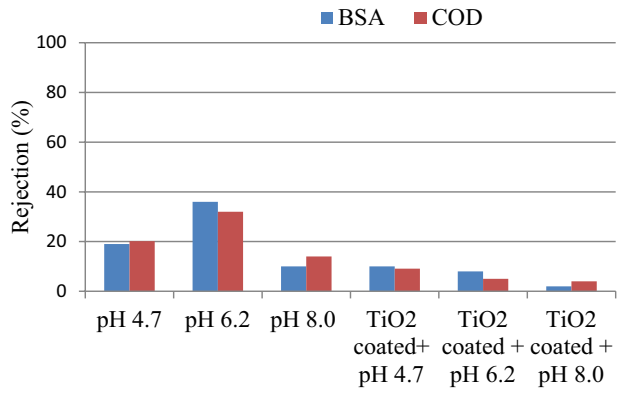

Fig. 10. Effect of pH on rejection at 100 kDa BSA filtration.

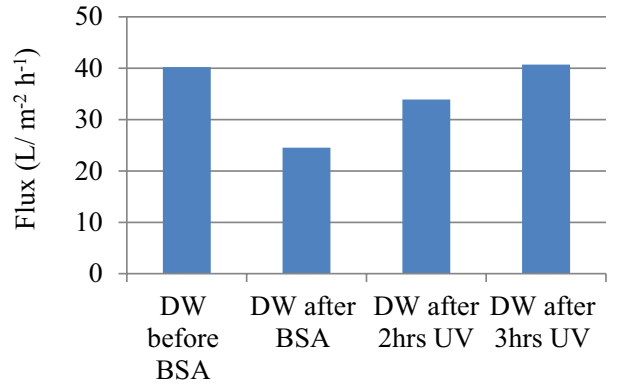

Fig. 11. Regeneration of BSA fouled 30 kDa membrane.

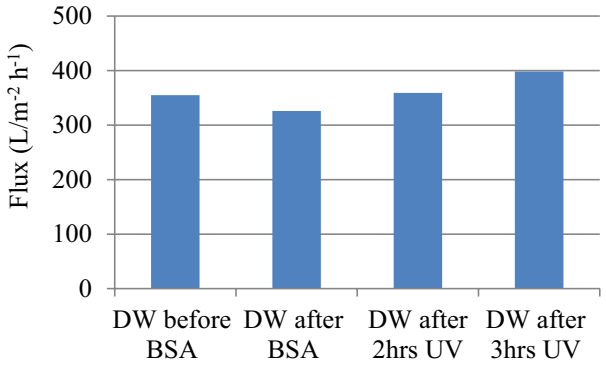

Fig. 12. Regeneration of BSA fouled 100 kDa membrane.

3.6. Regeneration of BSA fouled membrane via UV radiation

To check the cleanability of the membranes, after BSA filtration the fouled membranes were irradiated by UV (λ_{max} = 360 nm) light for 2 and 3 h. As indicated in Figs. 11 and 12, regeneration of 30 and 100 kD membrane surfaces fouled by BSA required 3 and 2 h UV exposure, respectively. However, long term irradiation may cause damage to the membrane, as is indicated by the increased water flux observed after 3 h of irradiation.

4. Conclusions

This work investigates the effects of TiO_2 covering PVDF polymeric membranes on the filtration and rejection of a model protein, BSA solution. The membrane modification produced a very hydrophilic membrane surface, as was proven by contact angle measurements on pristine and modified PVDF membranes, As TiO_2 makes the PVDF membrane very hydrophilic, the modification of the membrane surface may be a helpful strategy to control fouling. The photocatalytic regeneration of the fouled TiO_2 covered membrane by irradiation was also possible. Surprisingly, the modified 30 kD PVDF membrane demonstrated higher RM, moreover, the modified membrane showed lower BSA and COD rejection compared to the pristine membrane. Besides the presence of TiO_2 and the membrane MWCO, filtration resistances were affected by pH and the presence of phosphate-ions. The explanation of these results is not easy, as we have to take into consideration the protein-nanoparticle interactions. This is a very complex process, determined by several factors, such as electrostatic forces and hydrophobic dipol-dipol interactions. Although several work aimed at investigating BSA filtration through PVDF/TiO_2 composite membranes, in most cases the TiO_2 was embedded in the membrane material. Similarly to our results, slight flux decline [45] but improved BSA rejection were reported. Our results show, that the TiO_2 layer has different behavior. Although the exact description of the mechanisms of adsorption is not known, earlier results suggest that the surface of nanoparticles can modify the protein structure and therefore the behavior and function of the adsorbed proteins. As membrane modification via coupling with nanoparticles is a developing area, this phenomenon warrants more detailed investigation.

Acknowledgments

The authors would like to acknowledge the financial support of the Hungarian Science and Research Foundation (2017-2.3.7-TÉT-IN-2017-00016), the Hungarian State and the European Union (EFOP-3.6.2-16-2017-00010). Special thanks to Thomas Luxbacher for the Zeta-potential measurements.

References

[1] U.B. Deshannavar, R.K. Basavaraj, N.M. Naik, High rate digestion of dairy industry effluent by the up-flow anaerobic fixed-bed reactor, J. Chem. Pharm. Res., 4 (2012) 2895–2899.
[2] M.B.S. Shete, Comparative study of various treatments for dairy industry wastewater, IOSR J. Eng., 3 (2013) 42–47.
[3] S.S. Madaeni, Y. Mansourpanah, Screening membranes for COD removal from dilute wastewater, Desalination, 197 (2006) 23–32.
[4] L.Y.Ng, W.M. Abdul, P.L. Choe, H. Nidal, Polymeric membranes incorporated with metal/metal oxide nanoparticles: a comprehensive review, Desalination, 308 (2013) 15–33
[5] Y.R. Chang, Y.J. Lee, D.J. Lee, Membrane fouling during water or wastewater treatments: current research updated, J. Taiwan Inst. Chem. Eng., 94 (2018) 1–9.
[6] A. Asatekin, K. Seoktae, E. Menachem, M.M. Anne, Anti-fouling ultrafiltration membranes containing polyacrylonitrile-graft-poly(ethylene oxide) comb copolymer additives, J. Membr. Sci., 298 (2007) 136–46.
[7] M. Bellardita, R.G. Camera, V. Loddo, F. Parrino, L. Palmisano, Coupling of the membrane and photocatalytic technologies for selective formation of high added-value chemicals, Catal. Today, 340 (2018) 128–144.

[8] A. Vanangamudi, D. Saeki, L.F. Dumée, M. Duke, T. Vasiljevic, H. Matsuyama, X. Yang, Surface-engineered biocatalytic composite membranes for reduced protein fouling and self-cleaning, ACS Appl. Mater. Interfaces, 10 (2018) 27477–27487.
[9] M. Kokko, F. Bayerköhler, J. Erben, R. Zengerle, P. Kurz, S. Kerzenmacher, Molybdenum sulfides on carbon support as electrocatalysts for hydrogen evolution in acidic industrial wastewater, Appl. Energy, 190 (2017) 1221–1233.
[10] M. Kurian, D.S. Nair, Heterogeneous Fenton behavior of nano nickel-zinc ferrite catalysts in the degradation of 4-chlorophenol from water under neutral conditions, J. Water Process Eng., 8 (2015) e37–e49.
[11] J.L. Han, X. Xia, M.R. Haider, W.L. Jiang, Y. Tao, M.J. Liu, A.J. Wang, Functional graphene oxide membrane preparation for organics/inorganic salts mixture separation aiming at advanced treatment of refractory wastewater, Sci. Total Environ., 628–629 (2018) 261–270.
[12] S. Natarajan, D.S. Lakshmi, V. Thiagarajan, P. Mrudula, N. Chandrasekaran, A. Mukherjee, Antifouling and anti-algal effects of chitosan nanocomposite (TiO_2/Ag) and pristine (TiO_2 and Ag) films on marine microalgae *Dunaliella salina*, J. Environ. Chem. Eng., 6 (2018) 6870–6880.
[13] T. Das, X. Rocquefelte, R. Laskowski, L. Lajaunie, S. Jobic, P. Blaha, K. Schwarz, Investigation of the optical and excitonic properties of the visible light-driven photocatalytic $BiVO_4$ material, Chem. Mater., 29 (2017) 3380–3386.
[14] M. Li, G. Huang, Y. Qiao, J. Wang, Z. Liu, X. Liu, Y. Mei, Biocompatible and freestanding anatase TiO_2 nanomembrane with enhanced photocatalytic performance, Nanotechnology, 24 (2013) 305706.
[15] T. Hou, G. Dong, Y. Ye, V. Chen, Enzymatic degradation of bisphenol-A with immobilized laccase on TiO_2 sol-gel coated PVDF membrane, J. Membr. Sci., 469 (2014) 19–30.
[16] S. Ramasundaram, A. Son, M.G. Seid, S. Shim, S.H. Lee, Y.C Chung, S.W. Hong, Photocatalytic applications of paper-like poly(vinylidene fluoride)–titanium dioxide hybrids fabricated using a combination of electrospinning and electrospraying, J. Hazard. Mater., 285 (2015) 267–276.
[17] S. Ramasundaram, M.G. Seid, J.W. Choe, E.J Kim, Y.C. Chung, K. Cho, S.W. Hong, Highly reusable TiO_2 nanoparticle photocatalyst by direct immobilisation on steel mesh via PVDF coating, electrospraying, and thermal fixation, Chem. Eng. J., 306 (2016) 344–351.
[18] H.P. Ngang, B.S. Ooi, A.L. Ahmad, S.O. Lai, Preparation of PVDF–TiO_2 mixed-matrix membrane and its evaluation on dye adsorption and UV-cleaning properties, Chem. Eng. J., 197 (2012) 359–367.
[19] H. Song, J. Shao, Y. He, B. Liu, X. Zhong, Natural organic matter removal and flux decline with PEG–TiO_2-doped PVDF membranes by the integration of ultrafiltration with photocatalysis, J. Membr. Sci., 405–406 (2012) 48–56.
[20] M. Shaban, A.M. Ashraf, H. AbdAllah, H.M. Abd El-Salam, Titanium dioxide nanoribbons/multi-walled carbon nanotube nanocomposite blended polyethersulfone membrane for brackish water desalination, Desalination, 444 (2018) 129–141.
[21] Q. Wang, X. Wang, Z. Wang, J. Huang, Y. Wang, PVDF membranes with simultaneously enhanced permeability and selectivity by breaking the tradeoff effect via atomic layer deposition of TiO_2, J. Membr. Sci., 442 (2013) 57–64.
[22] I. Kovács, G. Veréb, S. Kertész, C. Hodúr, Z. László, Fouling mitigation and cleanability of TiO_2 photocatalyst-modified PVDF membranes during ultrafiltration of model oily wastewater with different salt contents, Environ. Sci. Pollut. Res., 25 (2018) 34912–34921.
[23] J. Aburabie, L.F. Villalobos, K.V. Peinemann, Composite membrane formation by combination of reaction-induced and nonsolvent-induced phase separation, Macromolec. Mater. Eng., 302 (2017) 1700131.
[24] J.P. Méricq, J. Mendret, S. Brosillon, C. Faur, High performance PVDF-TiO_2 membranes for water treatment, Chem. Eng. Sci., 123 (2015) 283–291.
[25] N. Nady, M.C.R. Franssen, H. Zuilhof, M.S. Mohy, R. Boom, K. Schroën, Modification methods for poly(arylsulfone) membranes: a mini-review focusing on surface modification, Desalination, 275 (2011) 1–9.
[26] L.T. Yogarathinam, A. Gangasalam, A.F. Ismail, S. Arumugam, A. Narayanan, The concentration of whey protein from cheese whey effluent using ultrafiltration by a combination of hydrophilic metal oxides and a hydrophobic polymer, J. Chem. Technol. Biotechnol., 93 (2018) 2576–2591.
[27] A. Di Mauro, M. Cantarella, G. Nicotra, G. Pellegrino, A. Gulino, M.V. Brundo, V. Privitera, G. Impellizzeri, Novel synthesis of ZnO/PMMA nanocomposites for photocatalytic applications, Sci. Rep., 7 (2017) 40895.
[28] K.H. Thebo, X. Qian, Q. Wei, Q. Zhang, H.M. Cheng, W. Ren, Reduced graphene oxide/metal oxide nanoparticles composite membranes for highly efficient molecular separation, J. Mater. Sci. Technol., 34 (2018) 1481–1486.
[29] A. Bottino, G. Capannelli, A. Comite, Preparation and characterisation of novel porous PVDF-ZrO_2 composite membranes, Desalination, 146 (2002) 35–40.
[30] L. Yan, Y.S. Li, C.B. Xiang, S. Xianda, Effect of nano-sized Al_2O_3-particle addition on PVDF ultrafiltration membrane performance, J. Membr. Sci., 276 (2006) 162–167.
[31] L. Yu, Z. Xu, H. Shen, H. Yang, Preparation and characterisation of PVDF – SiO_2 composite hollow fibre UF membrane by sol-gel method, J. Membr. Sci., 337 (2009) 257–265.
[32] M. Peyravi, M. Jahanshahi, S. Khalili, Fouling of WO_3 nanoparticle-incorporated PSf membranes in ultrafiltration of landfill leachate and dairy a combined wastewaters : An investigation using model, Chin. J. Chem. Eng., 25 (2017) 741–751.
[33] J. Kumar, A. Bansal, Photocatalysis by nanoparticles of titanium dioxide for drinking water purification: a conceptual and state-of-art review, Mater. Sci. Forum, 764 (2013) 130–150.
[34] S. Leong, A. Razmjou, K. Wang, K. Hapgood, X. Zhang, H. Wang, TiO_2 based photocatalytic membranes : a review, J. Membr. Sci., 472 (2014) 167–184.
[35] M.H.D.A. Farahani, V. Vatanpour, A comprehensive study on the performance and antifouling enhancement of the PVDF mixed matrix membranes by embedding different nanoparticulates: clay, functionalized carbon nanotube, SiO_2 and TiO_2, Sep. Purif. Technol., 197 (2018) 372–381.
[36] L. Hou, Z. Wang, P. Song, A precise combined complete blocking and cake filtration model for describing the flux variation in membrane filtration process with BSA solution, J. Membr. Sci., 542 (2017) 186–194.
[37] M. Hashino, K. Hirami, T. Ishigami, Y. Ohmukai, T. Maruyama, Effect of kinds of membrane materials on membrane fouling with BSA spinneret mixing nonsolvent injection coagulation bath, J. Membr. Sci., 384 (2011) 157–165.
[38] D. Zhao, S. Yu, A review of recent advance in fouling mitigation of NF/RO membranes in water treatment: pretreatment, membrane modification, and chemical cleaning, Desalin. Water Treat., 55 (2014) 870–891.
[39] N. Ismail, W.J. Lau, A.F. Ismail, P. Goh, Preparation and characterization of polysulfone/polyphenylsulfone/titanium dioxide composite ultrafiltration membranes for palm oil mill effluent treatment, Jurnal Teknologi, 65 (2013) 85–94.
[40] Y. Ding, B. Ma, H. Liu, J. Qu, Effects of protein properties on ultrafiltration membrane fouling performance in water treatment, J. Environ. Sci., 77 (2018) 273–281.
[41] S.R. Saptarshi, A. Duschl, A.L. Lopata, Interaction of nanoparticles with proteins: relation to bio-reactivity of the nanoparticle, J. Nanobiotechnol., 11 (2013) 26.
[42] Z. Xu, V.H. Grassian, Bovine serum albumin adsorption on TiO_2 nanoparticle surface : effects of pH and co-adsorption of phosphate on protein-surface interactions and protein structure, J. Phys. Chem. C, 121 (2017) 21763–21771.
[43] I.H. Huisman, P. Prádanos, A. Hernández, The effect of protein-protein and protein-membrane interactions on membrane fouling in ultrafiltration, J. Membr. Sci., 179 (2000) 79–90.
[44] M.T. Moghadam, G. Lesage, T. Mohammadi, J.-P. Mericq, J. Mendret, M. Heran, C. Faur, S. Brosillon, M. Hemmati, F. Naeimpoor, Improved antifouling properties of TiO_2/PVDF nanocomposite membranes in UV-coupled ultrafiltration, J. Appl. Polym. Sci., 132 (2015) 41731.